applicationS of Machine leArning to lhc Searches for cHarged mediator models and mineRal detectiOn searCheS for dark matter

SMASHROCS

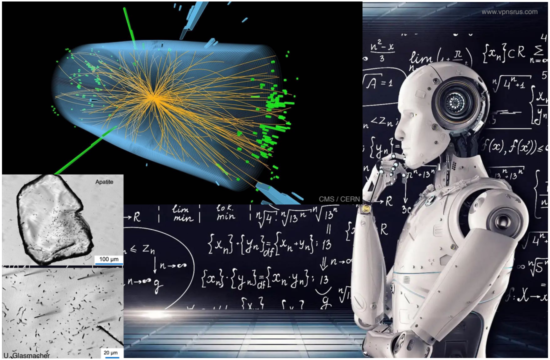

Jožef Stefan Institute
Ljubljana, Slovenia

SMASH
machine learning for science and humanities postdoctoral program

Co-funded by the European Union

This project has received funding from the European Union's Horizon Europe research and innovation programme under the Marie Skłodowska-Curie grant agreement No. 101081355.

Minimal extensions of the SM with a rich phenomenology

DM models with charged mediators

- SM singlet Majorana fermion DM
- Couples to SM through scalar partners of chiral fermions
- Produce mediators at colliders

Interactions similar to MSSM

$$\mathcal{L}_B \supset \lambda_R \tilde{\mu}_R^* \tilde{B} P_R \mu + \lambda_L \tilde{\mu}_L^* \tilde{B} P_L \mu$$

$$\mathcal{L}_\gamma \supset e \left(\tilde{\mu}_R^* \partial_\rho \tilde{\mu}_R + \tilde{\mu}_L^* \partial_\rho \tilde{\mu}_L \right) A^\rho$$

$$\mathcal{L}_W \supset g \left(\tilde{\nu}_\mu^* \partial_\rho \tilde{\mu}_L - \tilde{\mu}_L \partial_\rho \tilde{\nu}_\mu^* \right) W^\rho$$

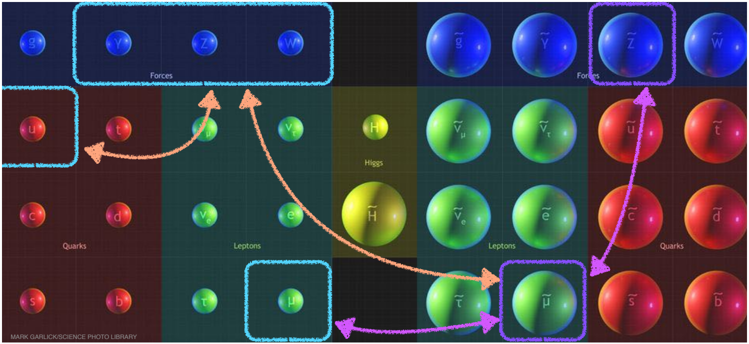

Generalize DM couplings to get $\Omega_{\rm DM}$ from DM annihilation

Fix $\theta_{\tilde{\mu}} = -45°$, $m_{\tilde{\mu}_2}/m_{\tilde{\mu}_1} = 1.25$

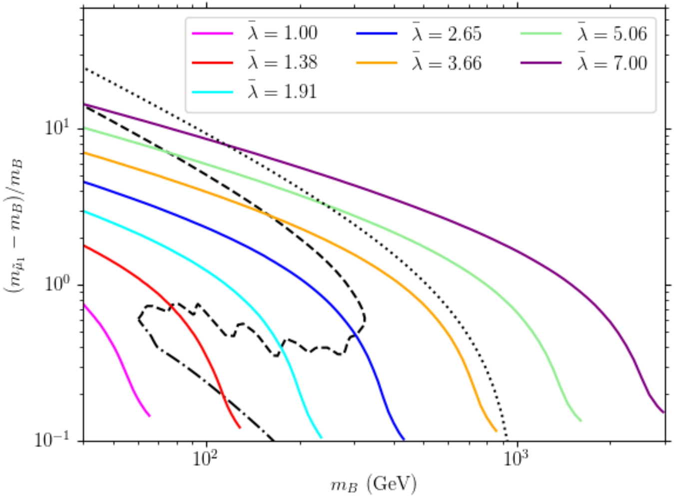

Charged mediator signals in proton collisions at LHC

- Protons composed of quarks, gluons
- SM interactions with mediators
- Decay to leptons and **invisible** DM

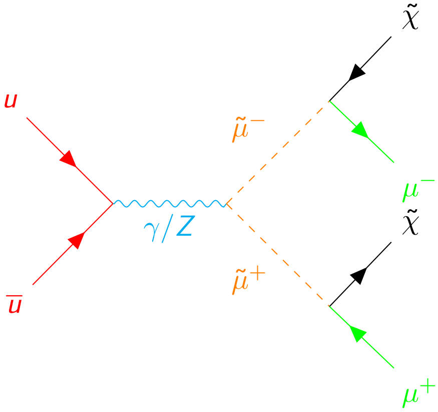

SM background process

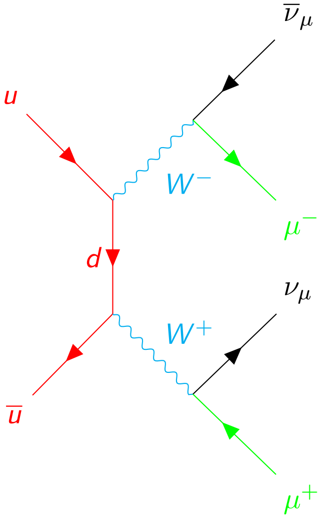

100x-1000x more likely

Search $pp \to \ell^+\ell^-\not{E}_T$ phase space for charged mediators

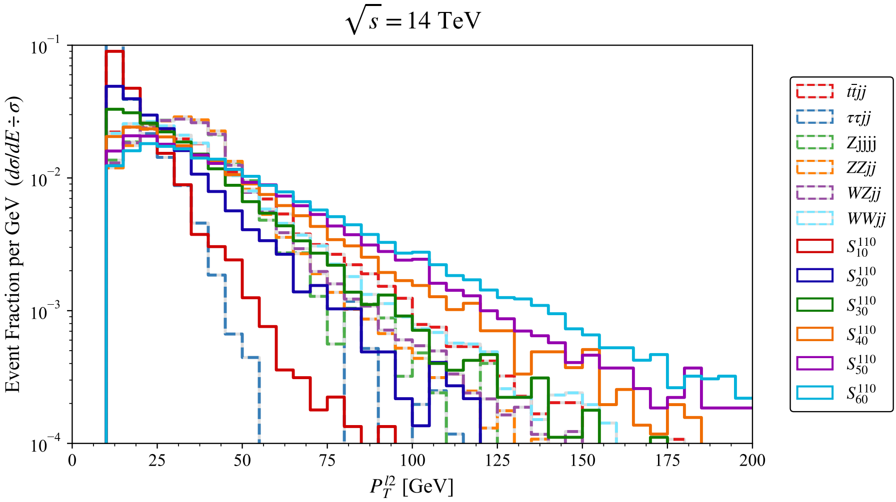

Project $\sim 3\sigma$ sensitivity to $m_{\tilde{\mu}_L} = 110\,\mathrm{GeV}$ at $\mathcal{L} = 300\mathrm{fb}^{-1}$

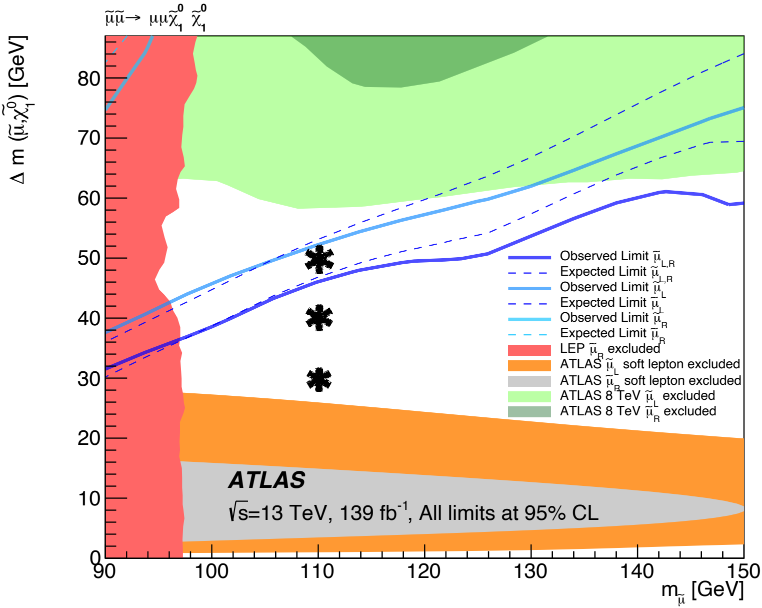

Trees partition final state phase space into decision regions

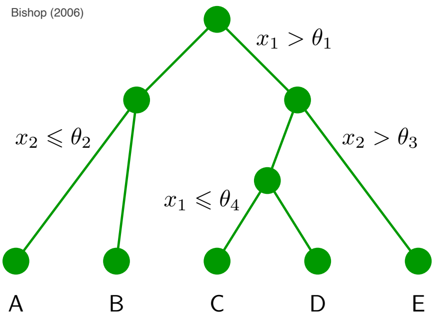

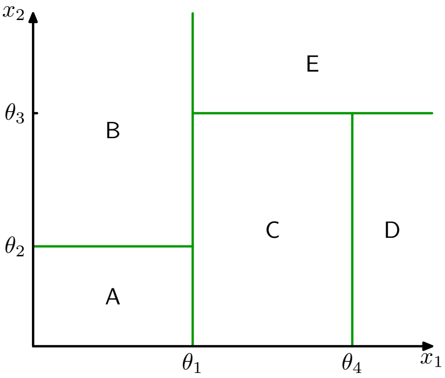

Split leaf nodes to minimize objective

$\mathrm{obj} = \sum_{\mathrm{data}} \ell(y_i, \hat{y}_i) + \omega(f)$, with $\hat{y}_i = f(\boldsymbol{x}_i)$ and regularization ω

Define tree by score on each leaf

$f(\boldsymbol{x}) = \boldsymbol{w}_{q(\boldsymbol{x})}$, vector of scores $\boldsymbol{w}$ with q assigning each $\boldsymbol{x}_i$ to a leaf

Ensembles of trees built iteratively using gradient boosting

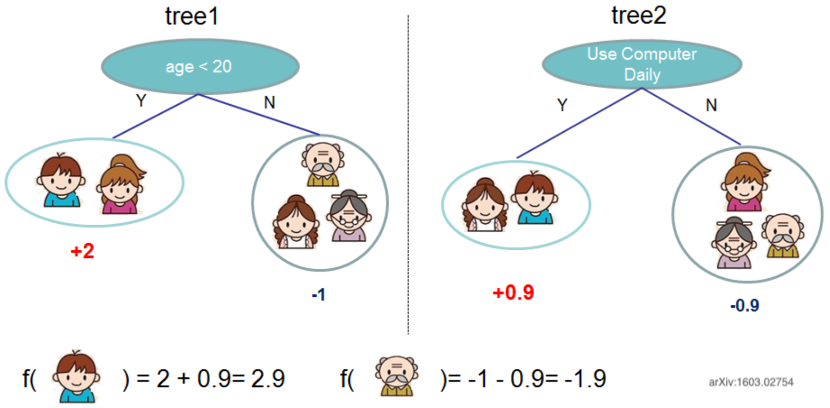

$$\hat{y}_i^{(t)} = \sum_{\text{trees}} f_j(\boldsymbol{x}_i) = \hat{y}_i^{(t-1)} + f_t(\boldsymbol{x}_i)$$

$$\text{obj} = \sum_{\text{data}} \ell(y_i, \hat{y}_i^{(t)}) + \omega(f_t)$$

$$\Delta\ell \approx \sum_{\text{data}} \left[g_i f_t(\boldsymbol{x}_i) + h_i f_t^2(\boldsymbol{x}_i)/2 \right]$$

$$g_i, h_i = \partial^{1,2}_{\hat{y}_i^{(t-1)}} \ell(y_i, \hat{y}_i^{(t-1)})$$

After precuts, train BDT to classify signal and background

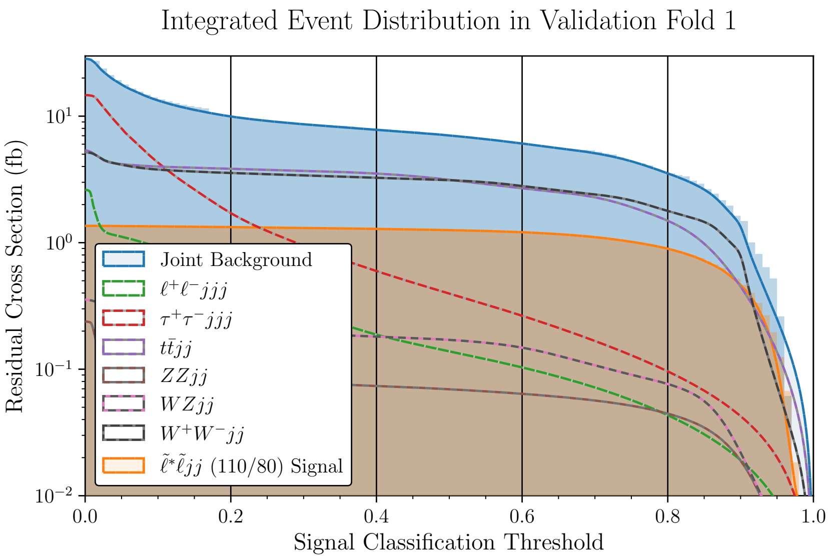

Significance $\gtrsim 6\sigma$ for $m_{\tilde{\mu}_L} = 110\,\mathrm{GeV}$ and $m_\chi = 80\,\mathrm{GeV}$

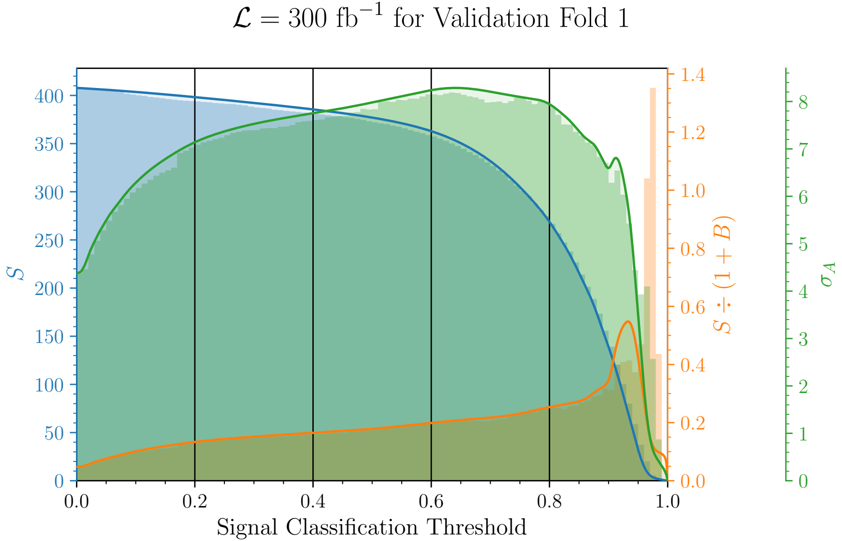

Discover $m_{\tilde{\mu}_L} \gtrsim 110\,\mathrm{GeV}$ and exclude $m_{\tilde{\mu}_L} \lesssim 160\,\mathrm{GeV}$

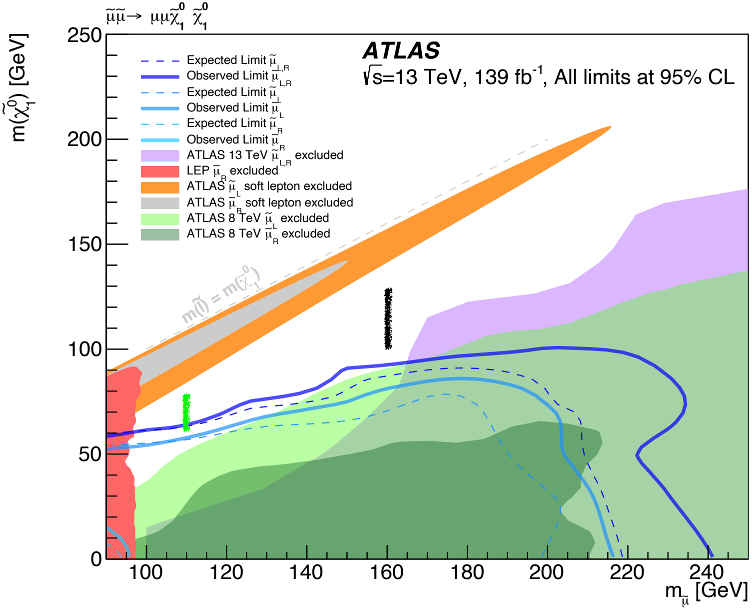

arXiv > astro-ph > arXiv:2301.07118

Search...

Help | Advanced

Astrophysics > Instrumentation and Methods for Astrophysics

[Submitted on 17 Jan 2023]

Mineral Detection of Neutrinos and Dark Matter. A Whitepaper

Sebastian Baum, Patrick Stengel, Natsue Abe, Javier F. Acevedo, Gabriela R. Araujo, Yoshihiro Asahara, Frank Avignone, Levente Balogh, Laura Baudis, Yilda Boukhtouchen, Joseph Bramante, Pieter Alexander Breur, Lorenzo Caccianiga, Francesco Capozzi, Juan I. Collar, Reza Ebadi, Thomas Edwards, Klaus Eitel, Alexey Elykov, Rodney C. Ewing, Katherine Freese, Audrey Fung, Claudio Galelli, Ulrich A. Glasmacher, Arianna Gleason, Noriko Hasebe, Shigenobu Hirose, Shunsaku Horiuchi, Yasushi Hoshino, Patrick Huber, Yuki Ido, Yohei Igami, Yoshitaka Itow, Takenori Kato, Bradley J. Kavanagh, Yoji Kawamura, Shingo Kazama, Christopher J. Kenney, Ben Kilminster, Yui Kouketsu, Yukiko Kozaka, Noah A. Kurinsky, Matthew Leybourne, Thalles Lucas, William F. McDonough, Mason C. Marshall, Jose Maria Mateos, Anubhav Mathur, Katsuyoshi Michibayashi, Sharlotte Mkhonto, Kohta Murase, Tatsuhiro Naka, Kenji Oguni, Surjeet Rajendran, Hitoshi Sakane, Paola Sala, Kate Scholberg, Ingrida Semenec, Takuya Shiraishi, Joshua Spitz, Kai Sun, Katsuhiko Suzuki, Erwin H. Tanin, Aaron Vincent, Nikita Vladimirov, Ronald L. Walsworth, Hiroko Watanabe

MDνDM community

- Groups across Europe, North America and Japan
- Astroparticle theorists, experimentalists, geologists, and materials scientists
- **MDνDM 2024** workshop in Washington DC in January

Check out our whitepaper!

- History of mineral detectors
- Review of scientific potential for particle physics, reactor neutrinos and geoscience
- Summary of active and planned experimental efforts

Damage tracks from nuclear recoils in ancient minerals

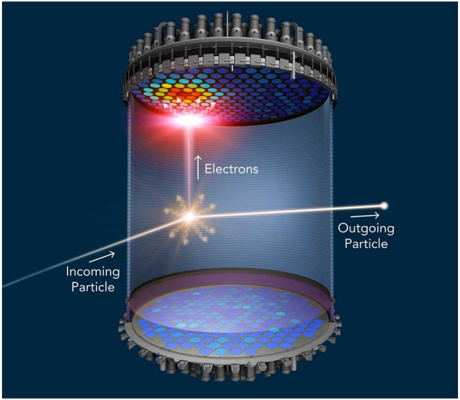

Figure: LUX-ZEPLIN (LZ) Collaboration / SLAC National Accelerator Laboratory

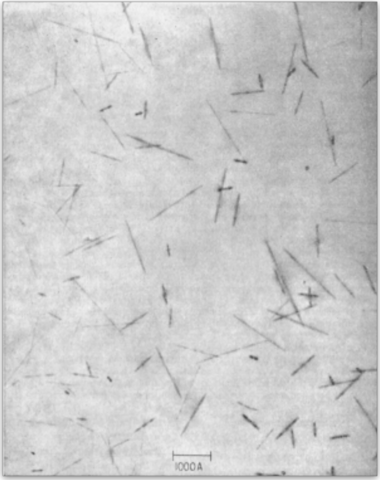

Figure: Price+Walker '63

New techniques allow for much larger readout capacity

Irradiation dose is 80 ions per field of view (20umx20um).

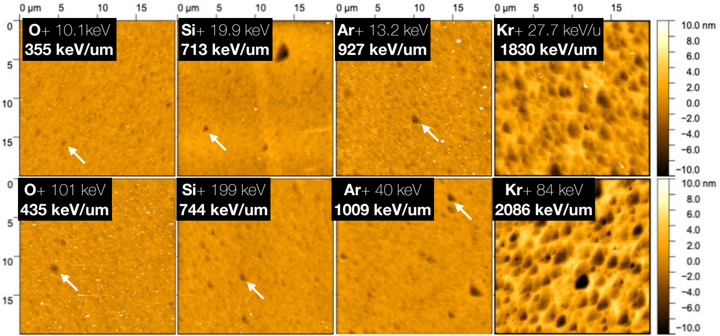

proxy	DM scattering	alpha recoils
pit formation efficiency	several to 10 %	~ 100%

Integrate stopping power to estimate track length

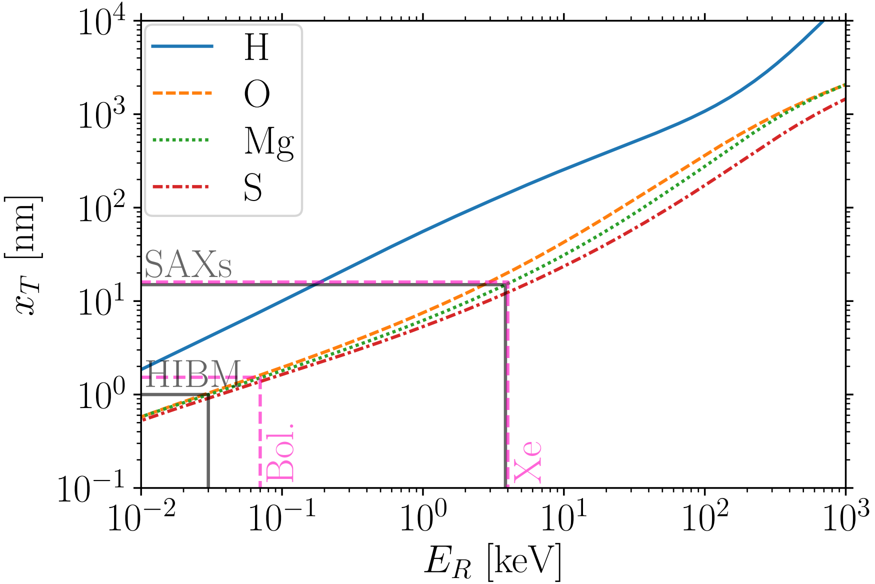

Cosmogenic backgrounds suppressed in deep boreholes

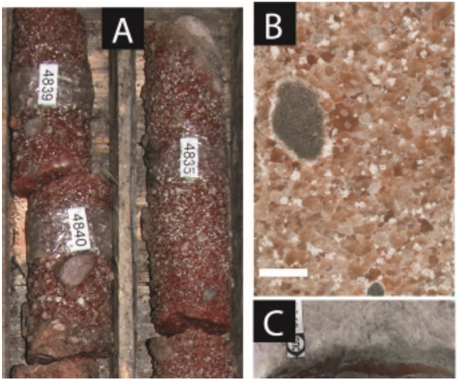

Figure: $\sim$ 2Gyr old Halite cores from $\sim$ 3km, as discussed in Blättler+ '18

Depth	Neutron Flux
2 km	$10^6/\mathrm{cm}^2/\mathrm{Gyr}$
5 km	$10^2/\mathrm{cm}^2/\mathrm{Gyr}$
6 km	$10/\mathrm{cm}^2/\mathrm{Gyr}$
50 m	$70/\mathrm{cm}^2/\mathrm{yr}$
100 m	$30/\mathrm{cm}^2/\mathrm{yr}$
500 m	$2/\mathrm{cm}^2/\mathrm{yr}$

Need minerals with low ^{238}U

- Marine evaporites with $C^{238} \gtrsim 0.01\,\mathrm{ppb}$
- Ultra-basic rocks from mantle, $C^{238} \gtrsim 0.1\,\mathrm{ppb}$

Recognition of sparse tracks is a data analysis challenge

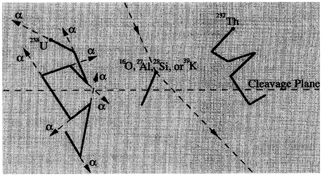

- 15 nm resolution of 100 g sample $\Rightarrow 10^{19}$ mostly empty voxels
- 1 Gyr old with $C^{238} = 0.01$ ppb $\Rightarrow 10^{13}$ voxels for α-recoil tracks

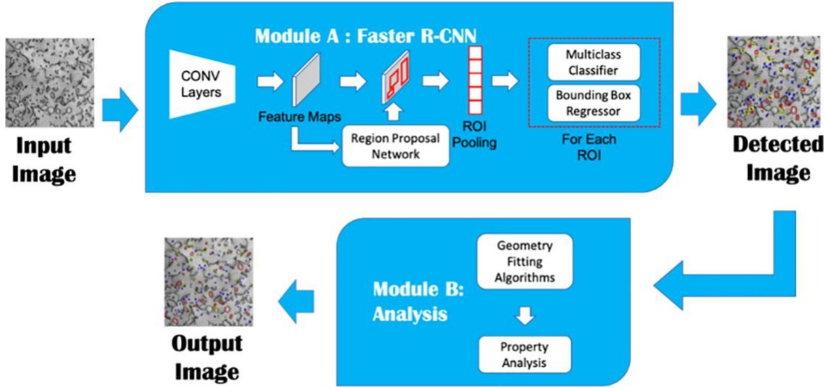

Use track length spectra to pick out WIMP signal

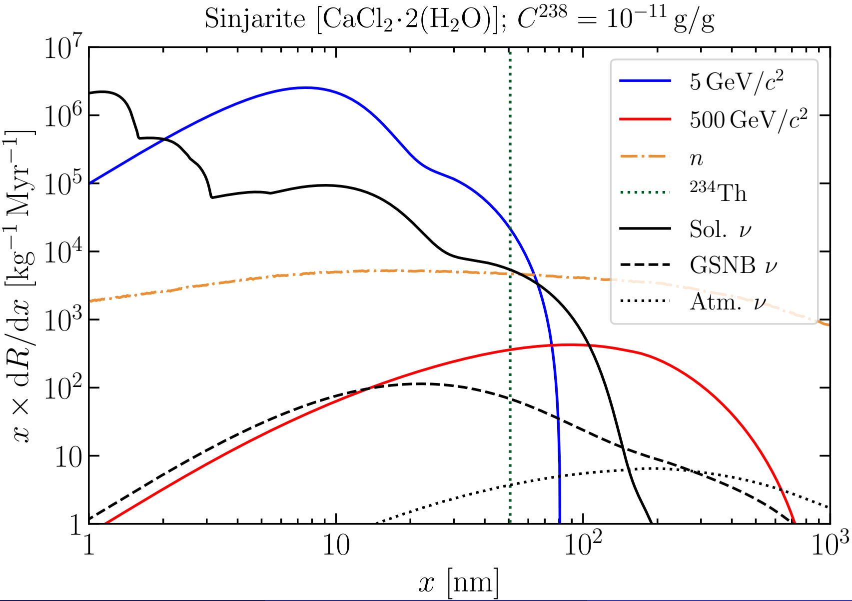

Trade-off between read-out resolution and exposure

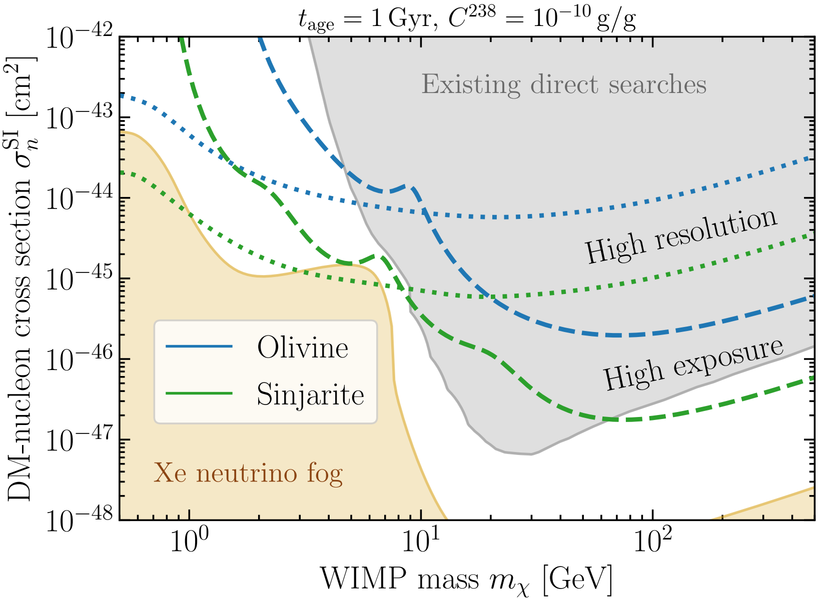

Use Machine Learning to probe the nature of Dark Matter

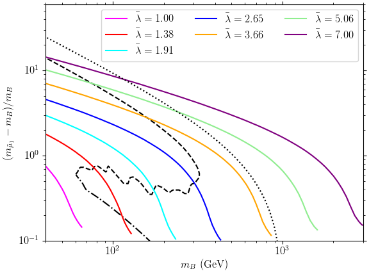

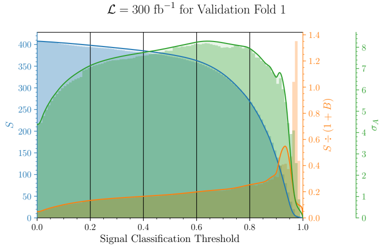

Improve on cut-and-count analysis for scalar lepton searches at LHC

- Sensitivity to $m_{\tilde{\mu}_L} \lesssim 160\,\mathrm{GeV}$
- Systematics $S/B \sim 0.15 - 0.40$
- Kinematic tranching to increase sampling at tails of distributions
- Precuts to bring signal and backgrounds (closer) to parity

Additional ML techniques

- Deep neural networks
- Convolutional neural networks
- Adversarial neural networks

Motivate/constrain parameter space by requiring $g_\mu - 2$

$$y = (m^2_{\tilde{\mu}_2} - m^2_{\tilde{\mu}_1}) \sin(2\theta_{\tilde{\mu}})/(4m^2_W)$$

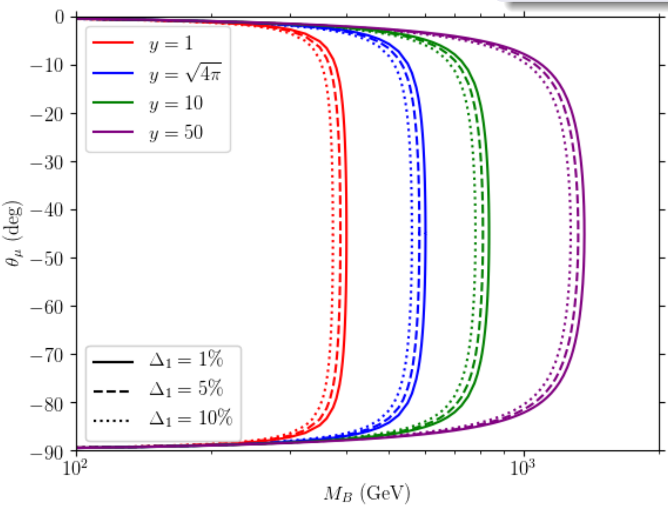

Parameter space for Δa_μ and Ω_{DM} from co-annihilation

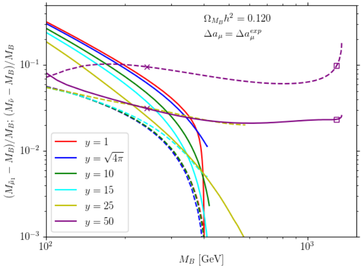

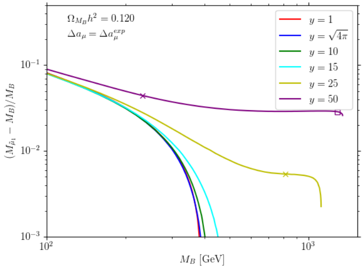

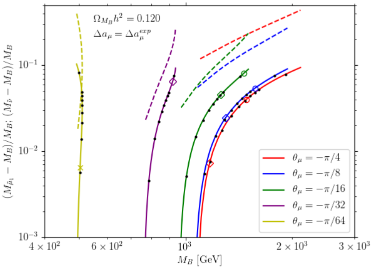

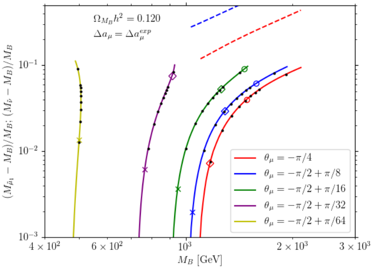

Perturbative unitarity and electroweak vacuum stability

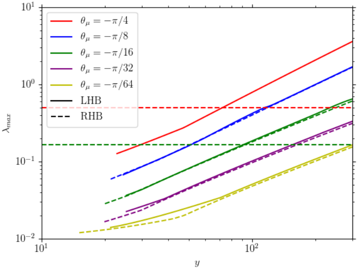

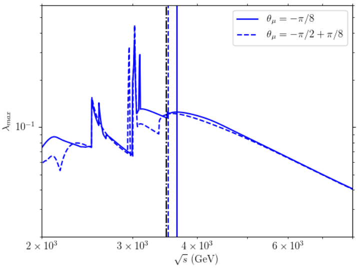

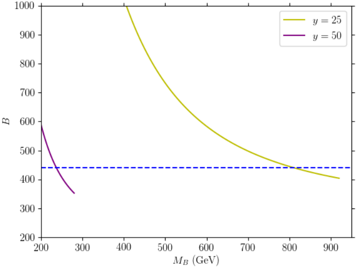

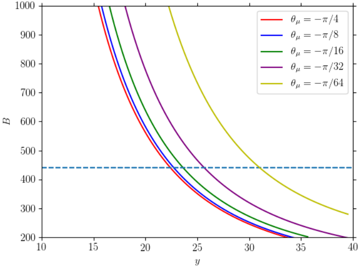

Simulation chain for new physics at LHC

Define Model
- Particle spectrum
- Feynman rules
- Parameter space

→

Parton Level
- Matrix elements
- Event simulation
- Sufficient statistics?

→

Hadron Level
- Parton showering
- Hadronization
- Jet Matching

→

Detector Level
- Fast simulation
- Reconstruction
- Phase space

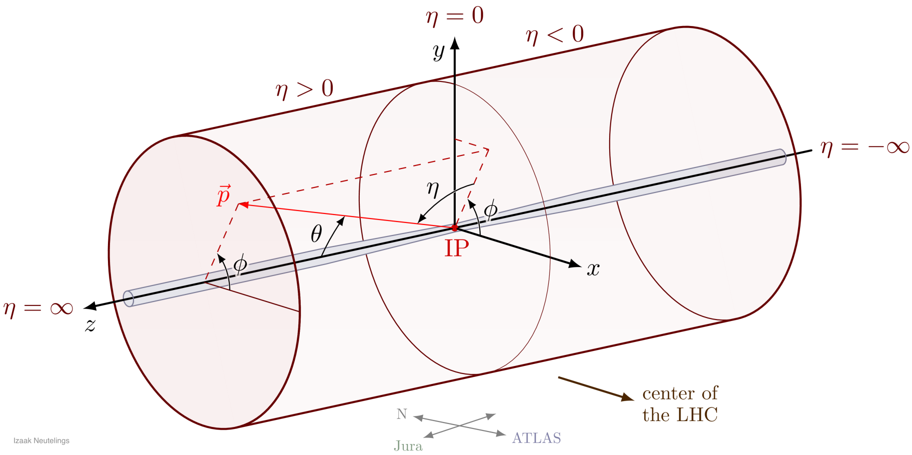

Construct higher level features

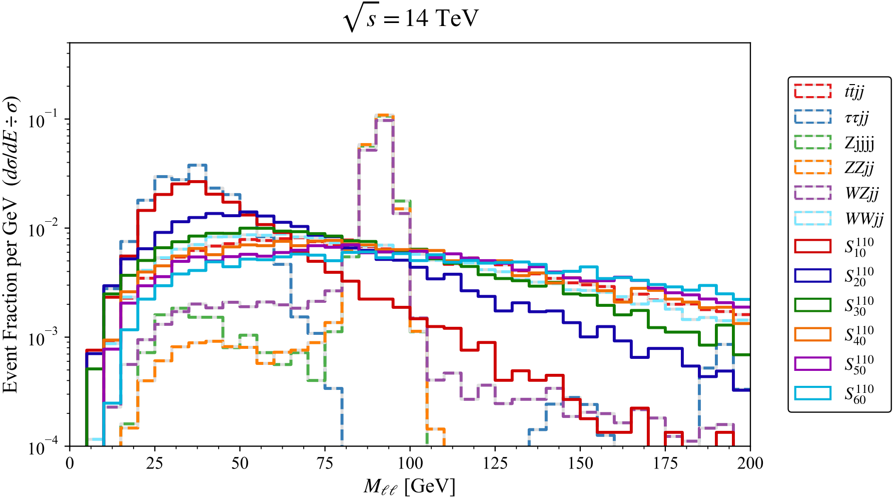

More kinematic distributions

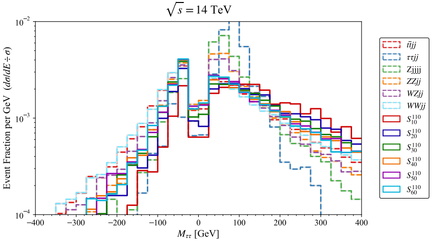

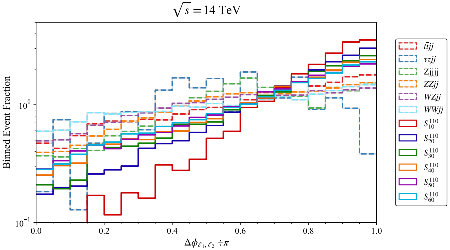

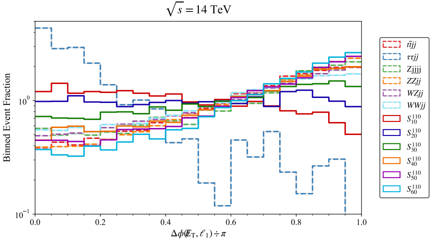

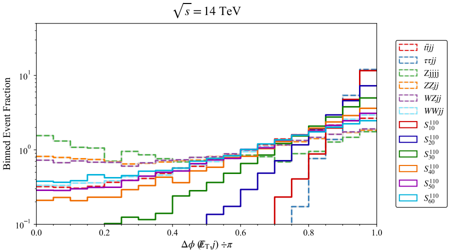

2D histograms of angular kinematic distributions

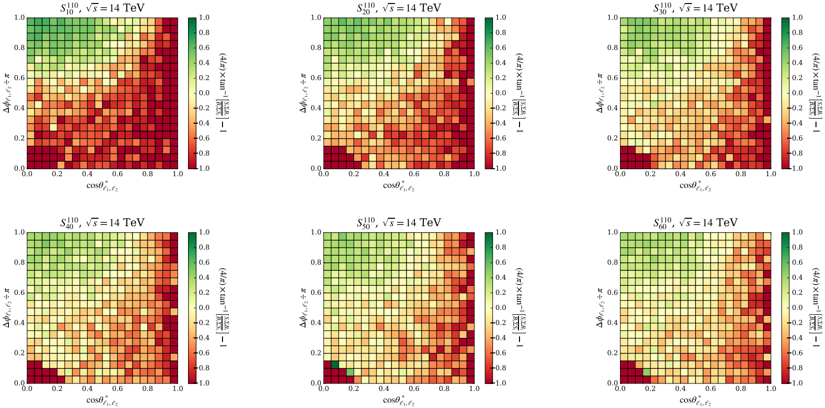

Residual cross sections (fb) for primary and secondary cuts

Primary Selection	$t\bar{t}jj$	$\tau\tau jj$	$Zjjjj$	$WWjj$	S_{30}^{110}	S_{40}^{110}
Matched Production	6.1×10^5	5.6×10^4	5.2×10^7	9.5×10^4	1.9×10^2	1.9×10^2
τ-veto	5.4×10^5	3.0×10^4	5.1×10^7	8.9×10^4	1.9×10^2	1.9×10^2
OSSF muon	3.5×10^3	4.3×10^2	6.0×10^5	5.1×10^2	8.1×10^1	8.8×10^1
exactly 1J $P_T > 30$	6.6×10^2	2.6×10^2	7.1×10^4	1.1×10^2	1.6×10^1	1.7×10^1
Jet b-veto	1.9×10^2	2.5×10^2	7.0×10^4	1.1×10^2	1.6×10^1	1.7×10^1
$\not{E}_T > 30$ GeV	1.6×10^2	1.8×10^2	8.9×10^3	9.2×10^1	1.3×10^1	1.4×10^1

Secondary Selection	$t\bar{t}jj$	$\tau\tau jj$	$Zjjjj$	$WWjj$	S_{30}^{110}	S_{40}^{110}
$m_{\ell\ell} \notin M_Z \pm 10$ GeV	1.4×10^2	1.8×10^2	6.2×10^2	7.9×10^1	1.1×10^1	1.2×10^1
$\cos\theta^*_{\ell_1,\ell_2} < 0.5$	8.1×10^1	1.6×10^2	4.7×10^2	4.5×10^1	8.0×10^0	9.0×10^0
$m_{\tau\tau} > 125$ GeV	2.7×10^1	2.3×10^1	8.7×10^1	1.4×10^1	3.6×10^0	3.9×10^0
$\not{E}_T > 125$ GeV	2.9×10^0	6.6×10^{-1}	0	2.3×10^0	6.6×10^{-1}	7.1×10^{-1}
Jet $P_T > 125$ GeV	1.1×10^0	6.6×10^{-1}	0	1.7×10^0	5.2×10^{-1}	4.6×10^{-1}

Tertiary cuts for optimized for intermediate mass gaps

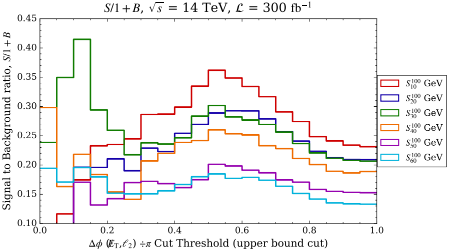

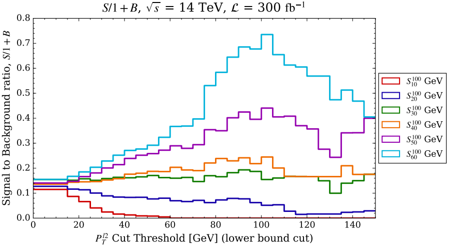

Tertiary Selection	$t\bar{t}jj$	$\tau\tau jj$	$WWjj$	S_{30}^{110}	S_{40}^{110}
$\Delta\phi(\ell_1,\ell_2) \div \pi > 0.5$	1.1×10^{0}	5.5×10^{-3}	1.3×10^{0}	4.4×10^{-1}	4.1×10^{-1}
$\Delta\phi(\not{E}_T,\ell_1) \div \pi < 0.6$	4.8×10^{-1}	5.5×10^{-3}	9.0×10^{-1}	3.3×10^{-1}	3.0×10^{-1}
$\Delta\phi(\not{E}_T,\ell_2) \div \pi < 0.6$	1.8×10^{-1}	0	5.1×10^{-1}	2.2×10^{-1}	2.0×10^{-1}
Events at $\mathcal{L} = 300$ fb^{-1}	52.8	0	151.7	66.0	60.0
$S \div (1+B)$	-	-	-	0.30	0.27
$S \div \sqrt{1+B}$	-	-	-	4.4	4.0

Additional folds for event distributions

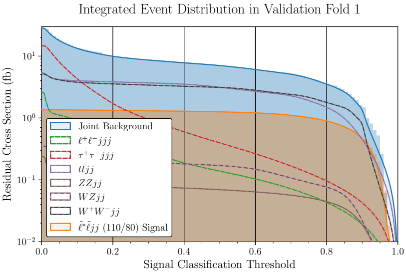

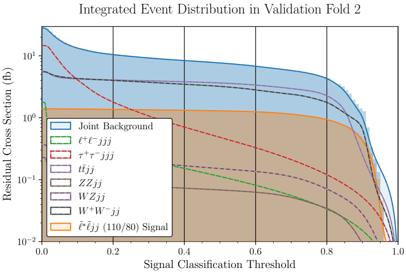

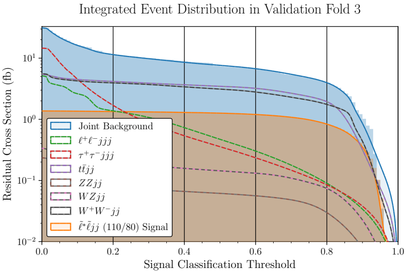

Additional folds for probability distributions

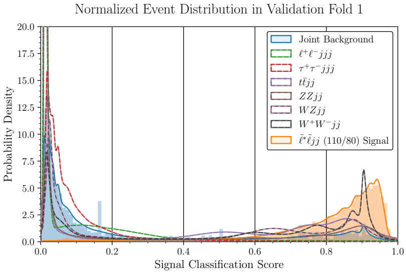

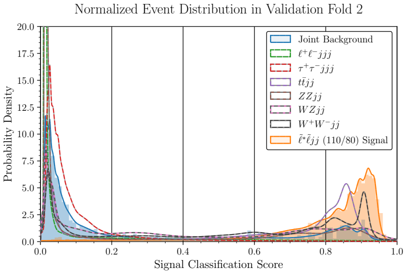

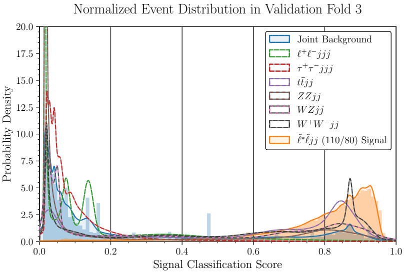

Additional folds for summary statistics

$\mathcal{L} = 300\ \text{fb}^{-1}$ for Validation Fold 1

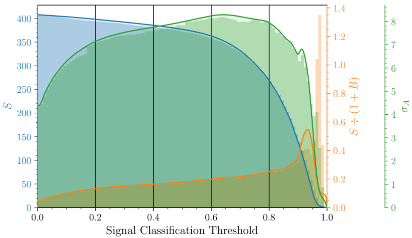

$\mathcal{L} = 300\ \text{fb}^{-1}$ for Validation Fold 2

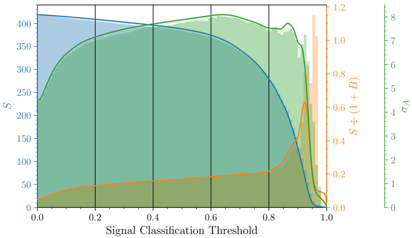

$\mathcal{L} = 300\ \text{fb}^{-1}$ for Validation Fold 3

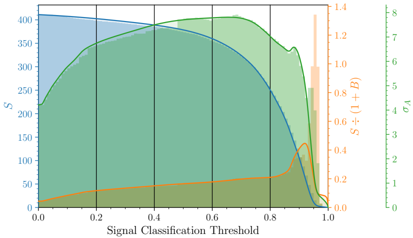

Features most important for BDT rejecting $t\bar{t}$, W^+W^-

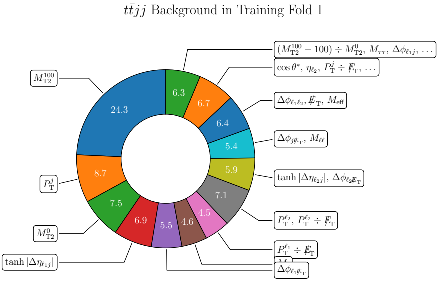

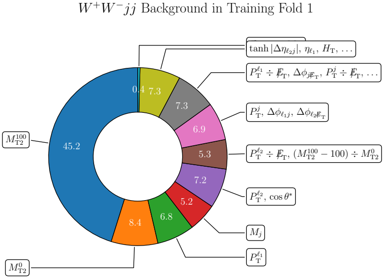

Relative contributions to reduction in ensemble objective function

- Sensitive to number of nodes
- Events through those nodes
- Weights carried by those events

M_{T2}^{100} dominates total gain for BDT trained for individual $t\bar{t}$, W^+W^-

Minimal mass of pair-produced parent to decay into $\ell + (\chi)(\nu)$ assuming $m_{\chi,\nu} = 100\,\mathrm{GeV}$

M_{T2}^{100} distribution for signal vs. $t\bar{t}$, W^+W^- after precuts

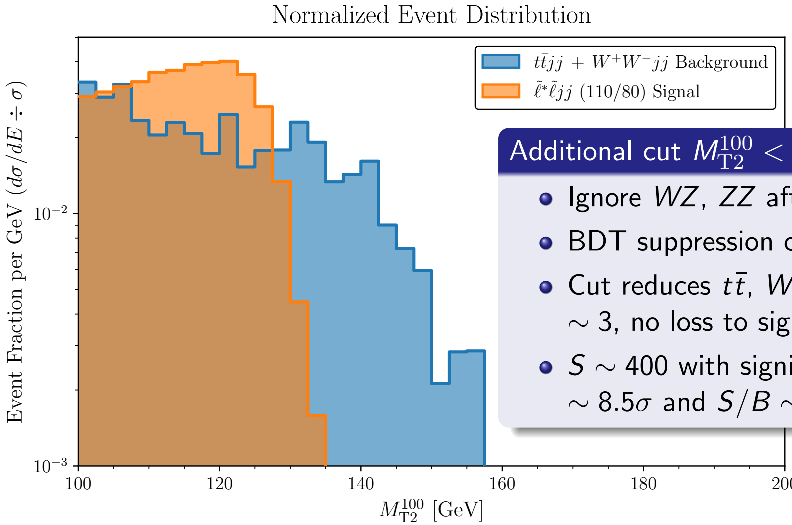

Additional cut $M_{\mathrm{T2}}^{100} < 130\,\mathrm{GeV}$

- Ignore WZ, ZZ after precuts
- BDT suppression of $\mu\mu$, $\tau\tau$
- Cut reduces $t\bar{t}$, W^+W^- by ~ 3, no loss to signal events
- $S \sim 400$ with significance $\sim 8.5\sigma$ and $S/B \sim 0.18$

Additional donut plots

$\ell^+\ell^- jjj$ Background in Training Fold 1

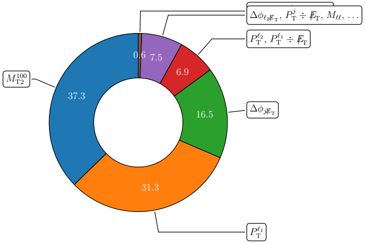

$\tau^+\tau^- jjj$ Background in Training Fold 1

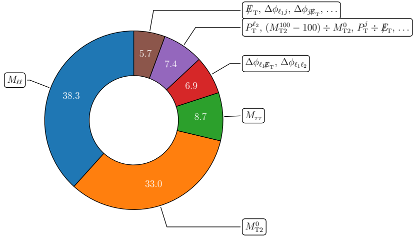

$ZZjj$ Background in Training Fold 1

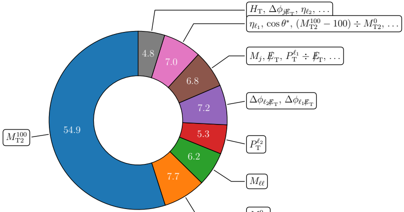

$WZjj$ Background in Training Fold 1

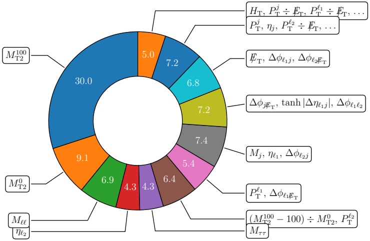

What do we (not) know about dark matter?

What we (typically) assume

- No E&M interactions
- Must be cold and stable
- Not in the Standard Model

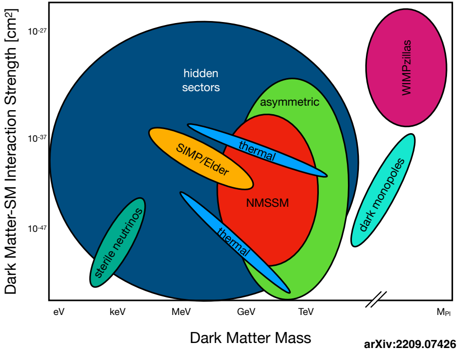

arXiv:2209.07426

Cleaving and etching limits ϵ and can only reconstruct 2D

Readout scenarios for different x_T

- HIBM+pulsed laser could read out 10 mg with nm resolution
- SAXs at a synchrotron could resolve 15 nm in 3D for 100 g

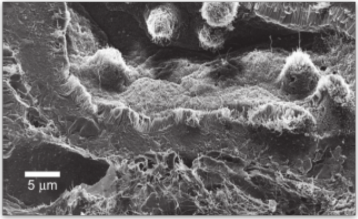

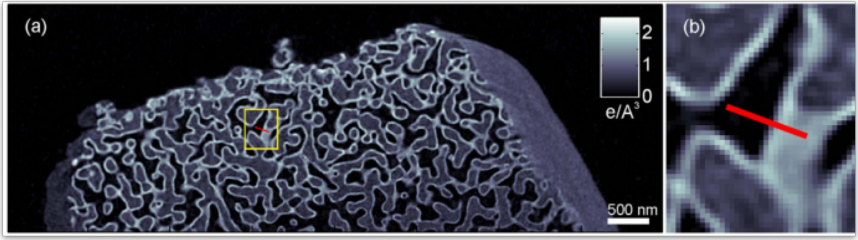

Figure: HIM rodent kidney Hill+ '12, SAXs nanoporous glass Holler+ '14

Find α-recoils and model radiogenic neutron background

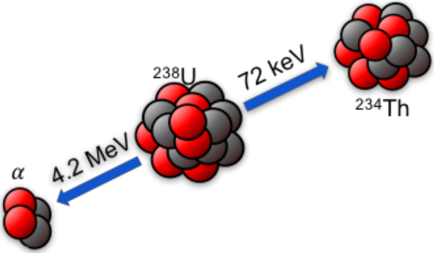

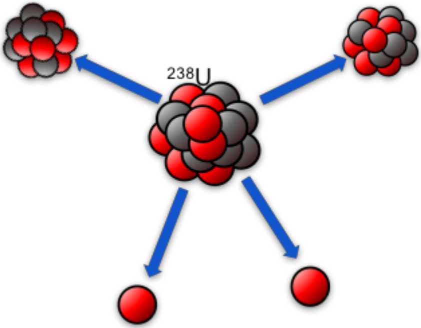

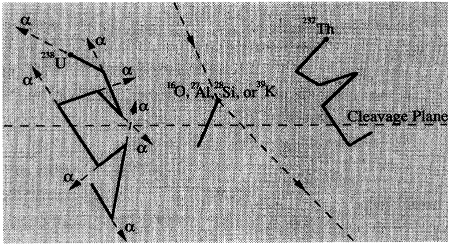

SF yields several $\sim$MeV neutrons

Each neutron will scatter elastically 10-1000 times before moderating

Scattering cross sections ⇒ scattering rates

$$\frac{d^2\sigma}{dq^2 d\Omega_q} = \frac{d\sigma}{dq^2}\frac{1}{2\pi}\delta\left(\cos\theta - \frac{q}{2\mu_{XT} v}\right) \simeq \frac{\sigma_0 F(q)^2}{8\pi\mu_{XT}^2 v}\delta\left(v\cos\theta - \frac{q}{2\mu_{XT}}\right)$$

$$\frac{d^2 R}{dE_R d\Omega_q} = 2M_T \frac{N_T}{M_T N_T}\int \frac{d^2\sigma}{dq^2 d\Omega_q} n_X\, v\, f(\boldsymbol{v}) d^3 v \simeq \frac{\sigma_0 F(q)^2}{4\pi\mu_{XT}} n_X \hat{f}(v_q, \hat{\boldsymbol{q}})$$

Differential cross section

- δ-function imposes kinematics
- σ_0 is velocity and momentum independent cross section for scattering off pointlike nucleus

$$F(q) \simeq \frac{9\left[\sin(qR) - qR\cos(qR)\right]^2}{(qR)^6}$$

Differential scattering rate

- Rate per unit time per unit detector mass for all nuclei
- Convolute cross section with astrophysical WIMP flux

$$\sigma_0^{SI} = \frac{4}{\pi}\mu_{XT}^2\left[Zf_s^p + (A-Z)f_s^n\right]^2$$

Nuclear recoils induced by elastic WIMP-nucleus scattering

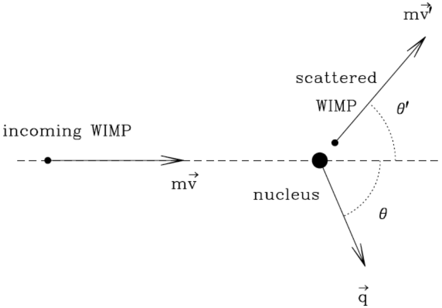

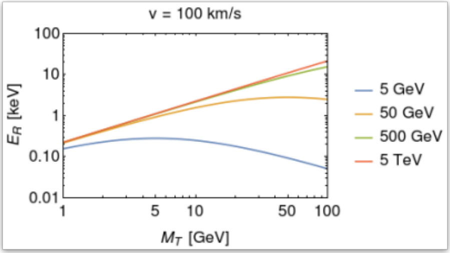

Rate per unit time per unit mass

$$\frac{dR}{dE_R} = \frac{n_X}{2}\frac{\sigma_{Xp}^{SI}}{\mu_{Xp}^2}A^2F(q)^2\eta(v_q)$$

Scattering kinematics ⇒ event rate

- Account for finite size of nucleus
- Convolute with WIMP flux
- Write cross section in terms of WIMP-nucleon interaction

WIMP velocity distribution and induced recoil spectra

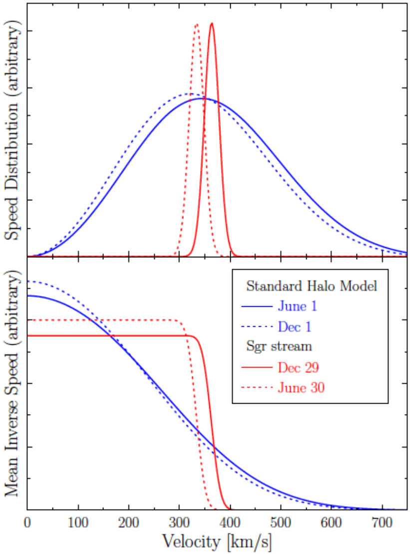

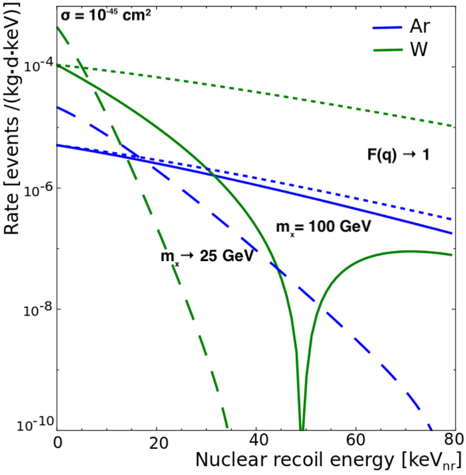

Figure: (left) 1209.3339 (right) 1509.08767

Mineral detectors used to constrain WIMPs before

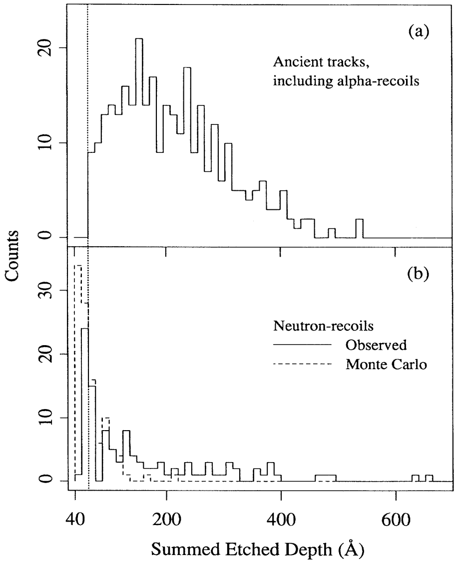

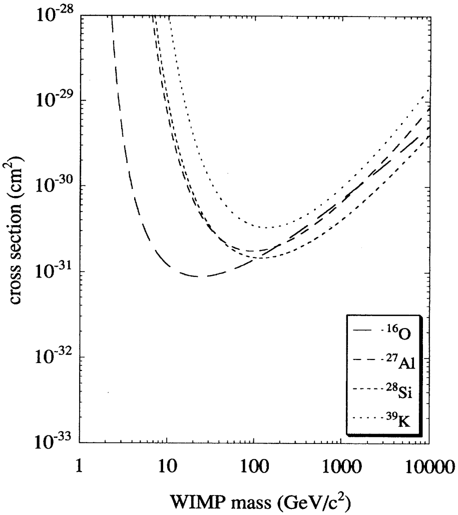

Figure: Snowden-Ifft et al. (1995)

Track length spectra after smearing by readout resolution

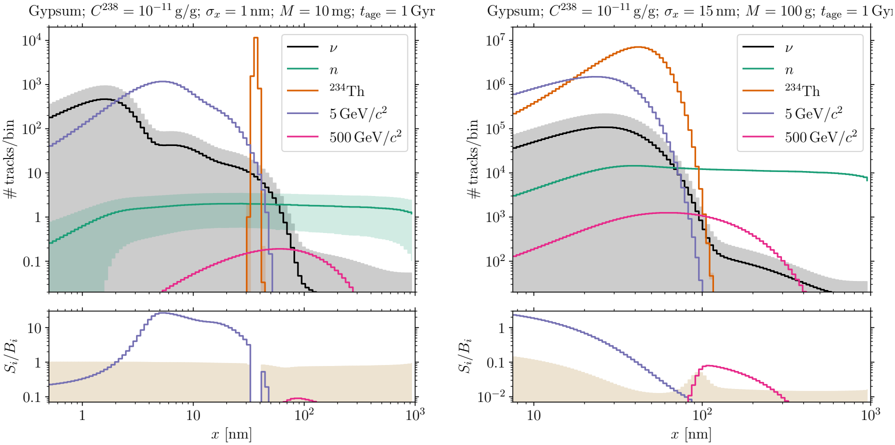

Sensitivity for different targets

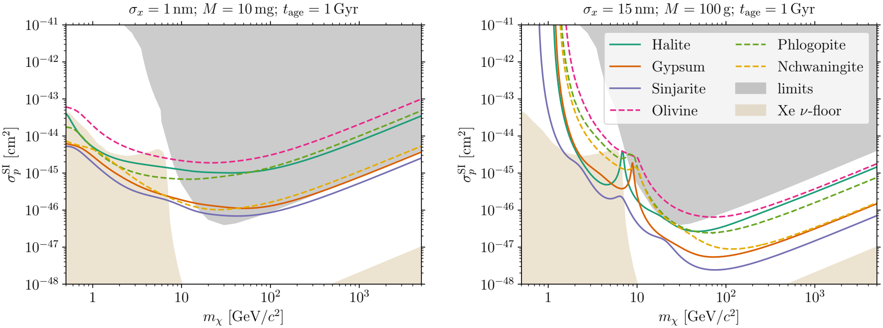

Halite	NaCl	$C^{238} = 10^{-11}$ g/g
Gypsum	$Ca(SO_4){\cdot}2(H_2O)$	$C^{238} = 10^{-11}$ g/g
Sinjarite	$CaCl_2{\cdot}2(H_2O)$	$C^{238} = 10^{-11}$ g/g
Olivine	$Mg_{1.6}Fe^{2+}_{0.4}(SiO_4)$	$C^{238} = 10^{-10}$ g/g
Phlogopite	$KMg_3AlSi_3O_{10}F(OH)$	$C^{238} = 10^{-10}$ g/g
Nchwaningite	$Mn^{2+}_2SiO_3(OH)_2{\cdot}(H_2O)$	$C^{238} = 10^{-10}$ g/g

Effects of background shape systematics

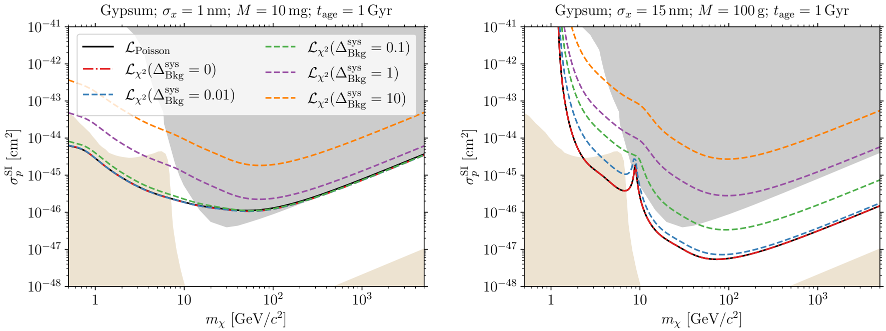

Sensitivity for different ^{238}U concentrations

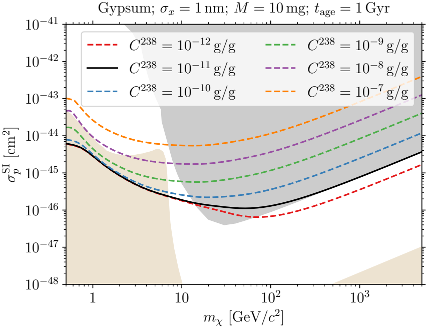

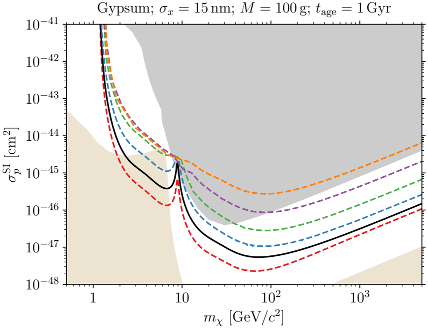

Multiple nuclei and large ϵ allow for optimal $\Delta m_X / m_X$

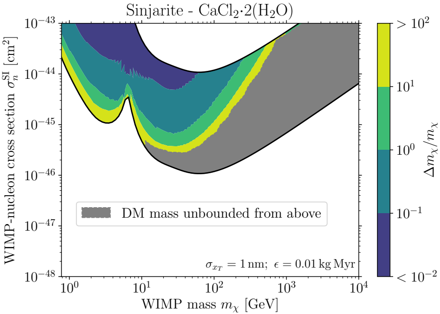

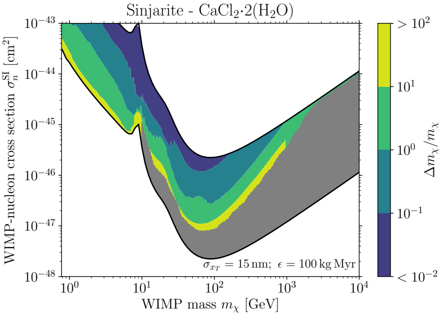

Mineral detectors can look for signals “averaged” over geological timescales or for time-varying signals

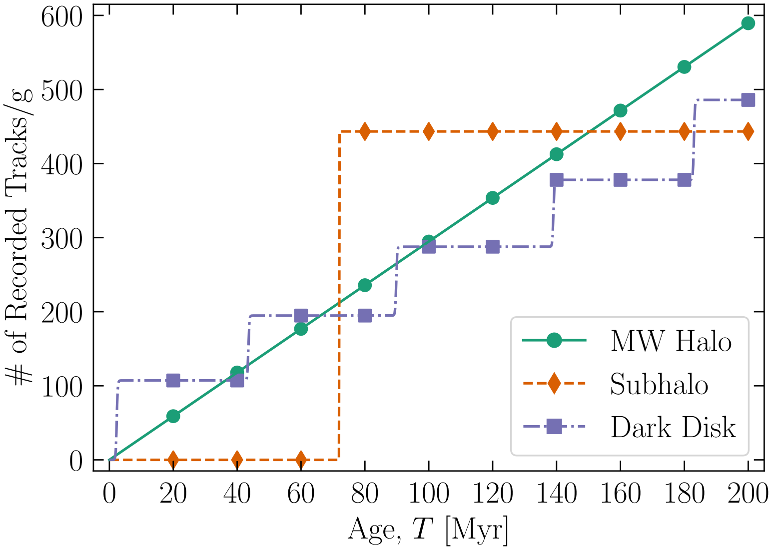

Multiple samples to detect dark disk transit every ~ 45 Myr

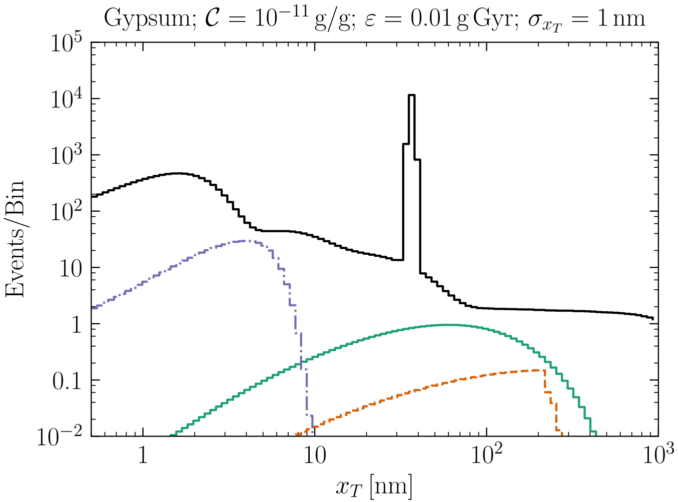

$m_X^{\rm disk} = 100$ GeV $\sigma_{Xp}^{\rm disk} = 10^{-43}\,{\rm cm}^2$ $m_X = 500$ GeV $\sigma_{Xp} = 5 \times 10^{-46}\,{\rm cm}^2$

Distinguish from halo with 20, 40, 60, 80, 100 Myr samples

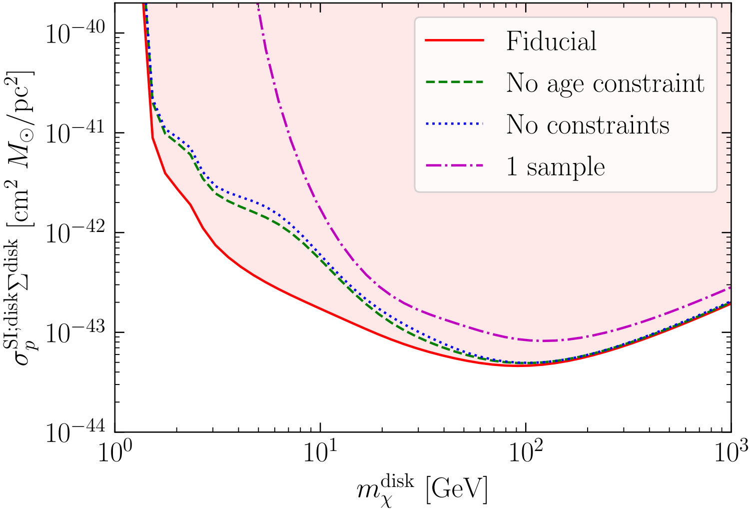

Systematic uncertainties $\Delta_t = 5\%$ $\Delta_M = 0.1\%$ $\Delta_C = 10\%$ $\Delta_\Phi = 100\%$

Change number of samples and sample spacing in time

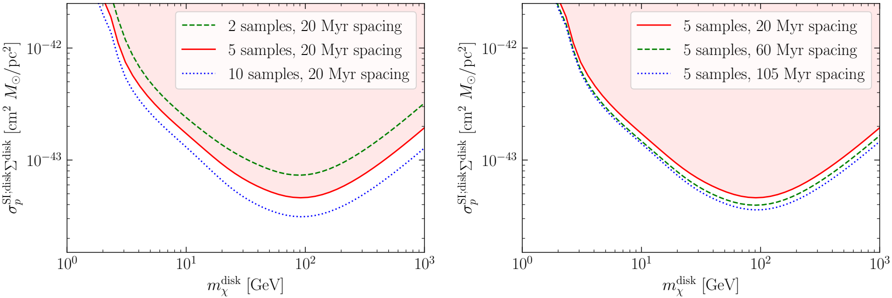

Neutrinos come from a variety of sources

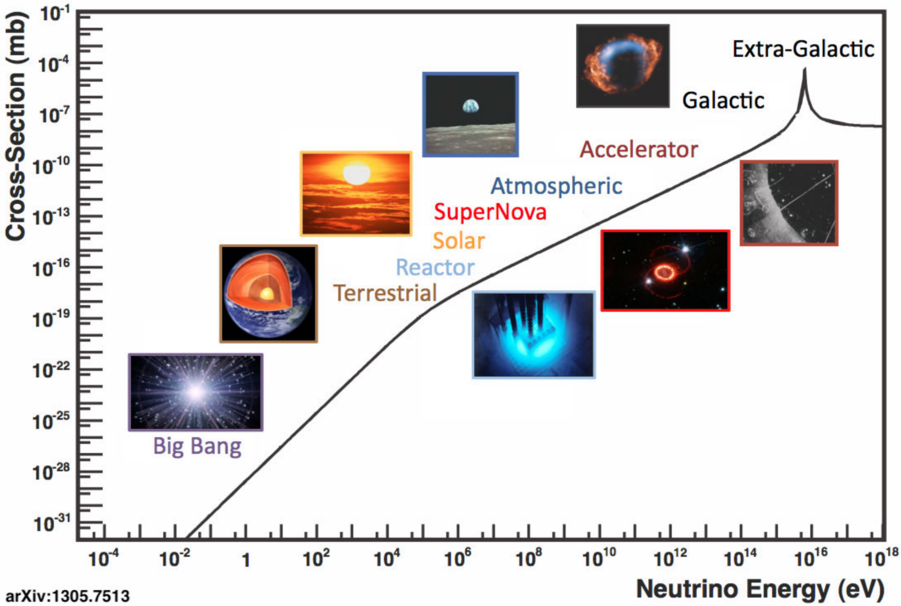

Nuclear recoil spectrum depends on neutrino energy

$$\frac{dR}{dE_R} = \frac{1}{m_T} \int dE_\nu \, \frac{d\sigma}{dE_R} \frac{d\phi}{dE_\nu}$$

- Quasi-elastic for $E_\nu \gtrsim 100\,\text{MeV}$
- Resonant π production at $E_\nu \sim \text{GeV}$
- Deep inelastic for $E_\nu \gtrsim 10\,\text{GeV}$

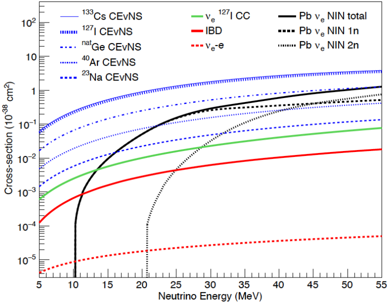

Figure: COHERENT, 1803.09183

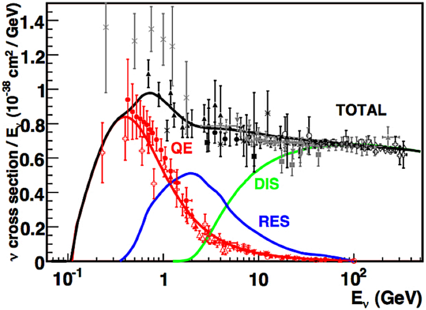

Figure: Inclusive CC $\sigma_{\nu N}$, 1305.7513

Atmospheric ν's originating from CR interactions

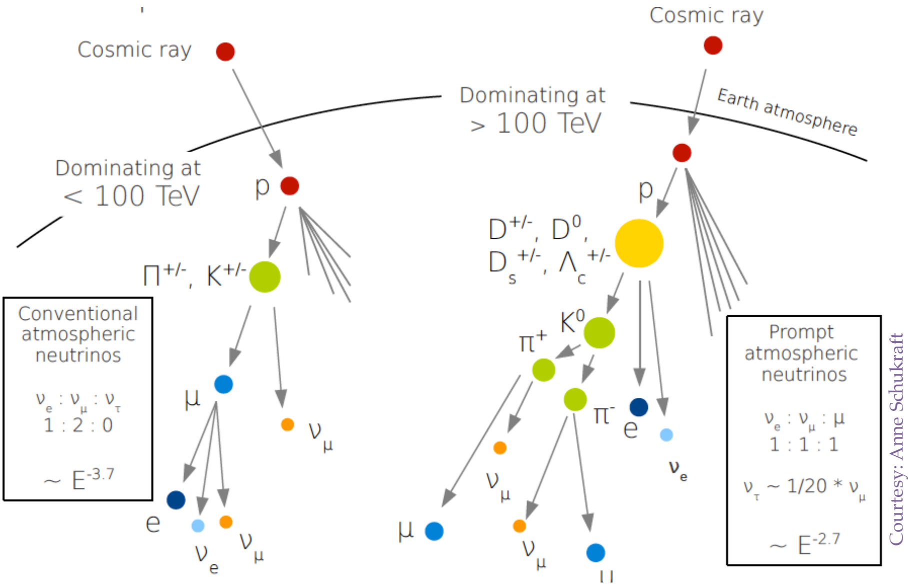

Atmospheric ν's originating from CR interactions

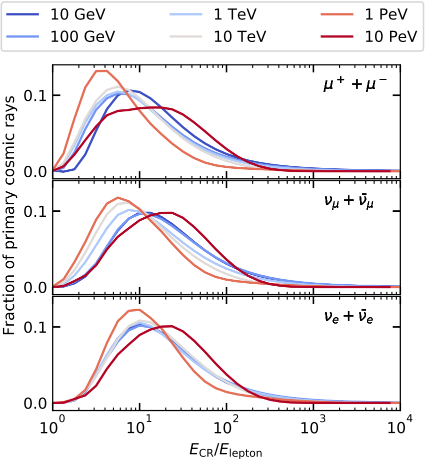

Figure: E_{CR} to leptons, 1806.04140

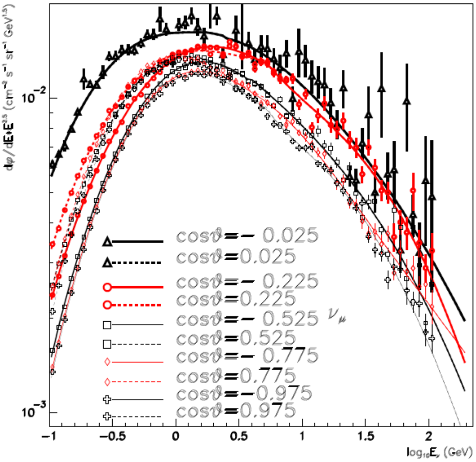

Figure: FLUKA simulation of ν_μ flux at SuperK for solar max, hep-ph/0207035

Geomagnetic field deflects lower energy CR primaries

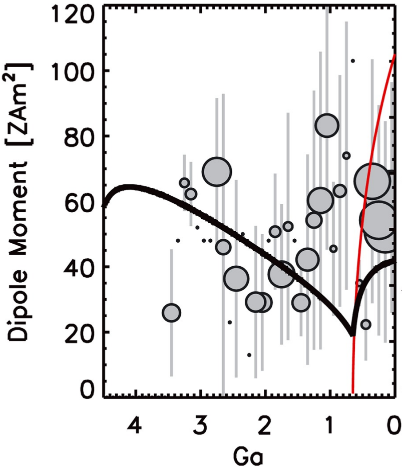

Figure: Driscoll, P. E. (2016), *Geophys. Res. Lett.*, 43, 5680-5687

Rigidity $p_{CR}/Z_{CR} \simeq E_{CR}$ for CR protons

- Rigidity cutoff $\propto M_{dip}$ truncates atmospheric ν spectrum at low E_ν
- Maximum cutoff today $\sim 50\,\mathrm{GV}$
- Recall CR primary $E_{CR} \gtrsim 10\,E_\nu$

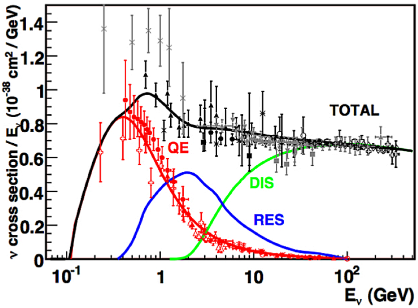

Recoil spectra from atmospheric ν's incident on NaCl(P)

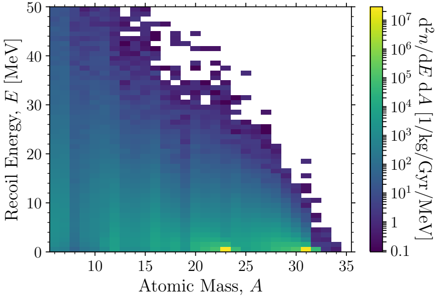

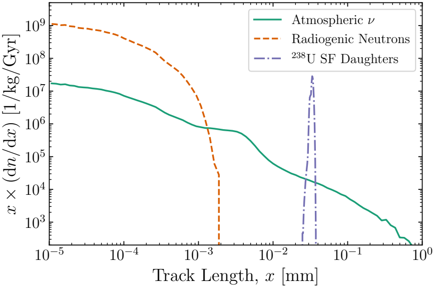

Recoils of many different nuclei

- Low energy peak from QE neutrons scattering ^{23}Na, ^{31}P
- High energy tail of lighter nuclei produced by DIS

Background free regions for $\gtrsim 1\,\mu$m

- Radiogenic n-bkg confined to low x, regardless of target
- Subdominant systematics from atmosphere, heliomagnetic field

Galactic contribution to ν flux over geological timescales

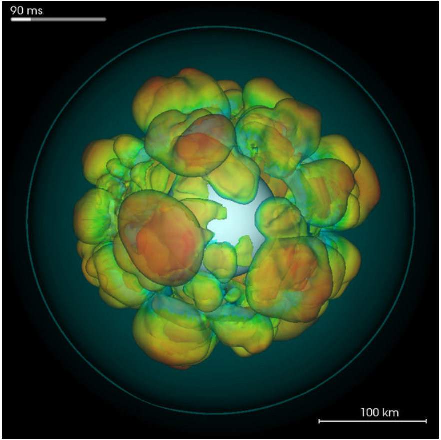

Figure: Supernova simulation after CC

Only $\sim$ 2 SN 1987A events/century

- Measure galactic CC SN rate
- Traces star formation history

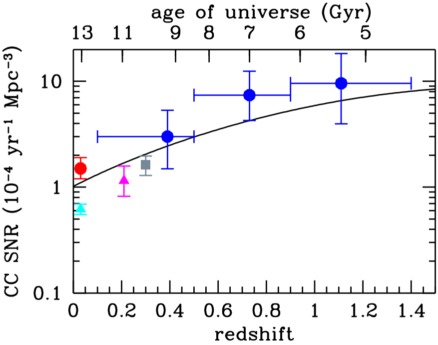

Figure: Cosmic CC SNR, 1403.0007

Galactic contribution to ν flux over geological timescales

$$\frac{\mathrm{d}\phi}{\mathrm{d}E_\nu} = \dot{N}_{\mathrm{CC}}^{\mathrm{gal}} \frac{\mathrm{d}n}{\mathrm{d}E_\nu} \int_0^\infty \mathrm{d}R_E \frac{f(R_E)}{4\pi R_E{}^2}$$

Only $\sim$ 2 SN 1987A events/century

- Measure galactic CC SN rate
- Traces star formation history

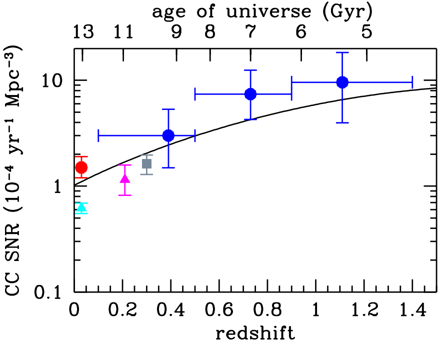

Figure: Cosmic CC SNR, 1403.0007

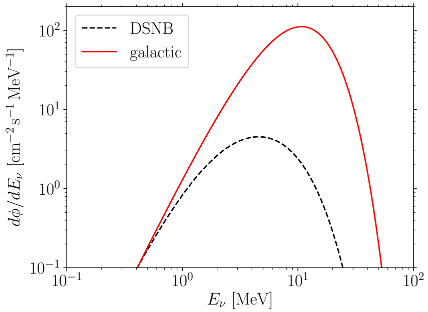

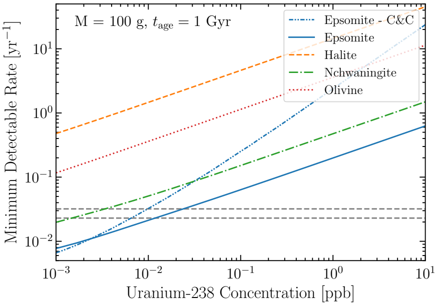

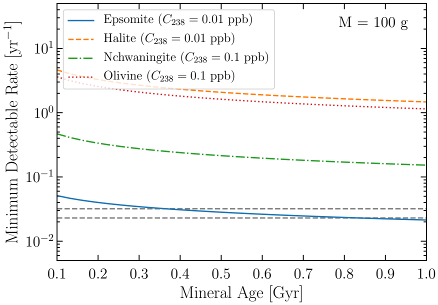

Epsomite [$Mg(SO_4)\cdot 7(H_2O)$]
Halite [NaCl]

Nchwaningite [$Mn_2^{2+}SiO_3(OH)_2\cdot(H_2O)$]
Olivine [$Mg_{1.6}Fe_{0.4}^{2+}(SiO_4)$]

Difficult to pick out time evolution of galactic CC SN rate

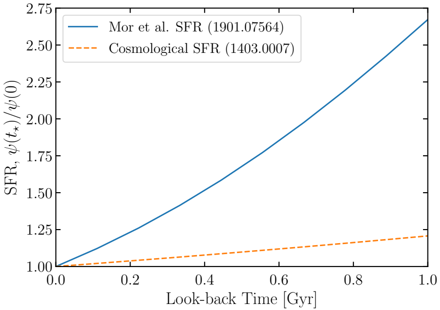

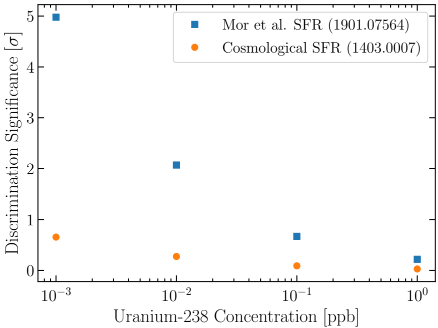

Coarse grained cumulative time bins

- 10 Epsomite paleo-detectors
- 100 g each, $\Delta t_{\rm age} \simeq 100$ Myr

Determine σ rejecting constant rate

Could only make discrimination at 3σ for $\mathcal{O}(1)$ increase in star formation rate with $C^{238} \lesssim 5$ ppt

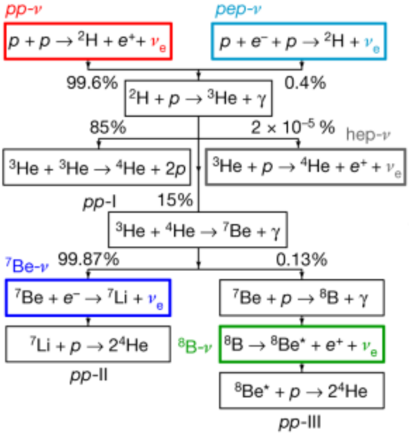

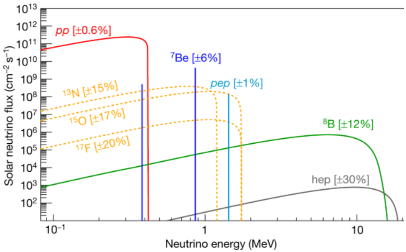

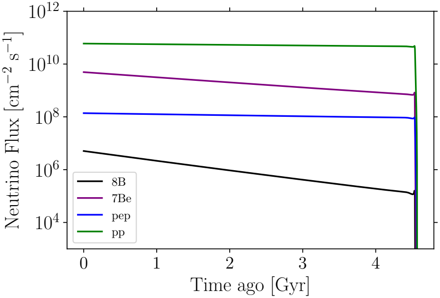

Figure: Today's flux at Borexino (Nature, 2018) and time dependence of GS metallicity model, 2102.01755

Could use large exposure to differentiate between scenarios

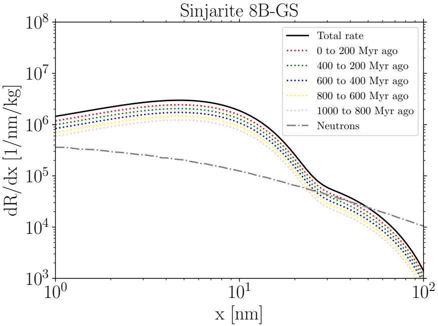

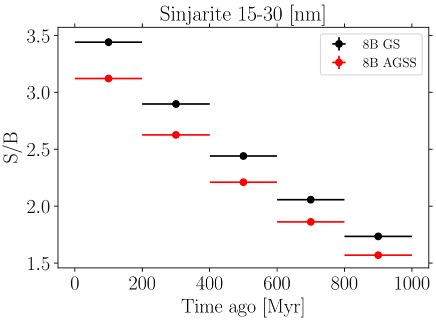

Could measure ^8B flux over time

- Higher $E_\nu \Rightarrow$ longer tracks
- Highly dependent on solar core temperature with flux $\propto T^{24}$
- Sensitive to metallicity model

100 g samples with 15 nm resolution

- Look in single bin $15 - 30$ nm
- Assume $\Delta_t \sim 10\%$, $\Delta_C = 10\%$
- $N_{\rm tot}^{\rm GS} \sim (1.63 \pm 0.05) \times 10^6$
  $N_{\rm tot}^{\rm AGSS} \sim (1.52 \pm 0.05) \times 10^6$

Reactor ν's produced in β decays of fission fragments

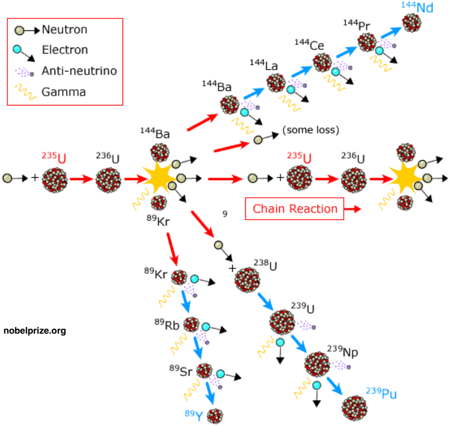

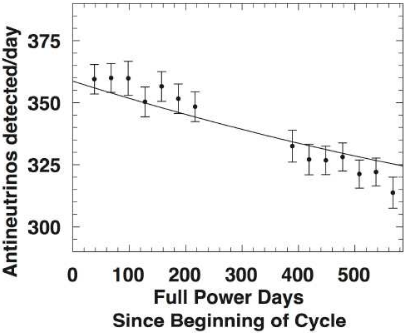

Figure: Processes yielding reactor ν's and time dependence over the course of reactor fuel cycle for $^{239}\mathrm{Pu}$ (1605.02047)

Nuclear non-proliferation safeguards

- Measure soft nuclear recoils
- Passive and robust detectors operable at room temperature

Semi-analytic range calculations and SRIM agree with data

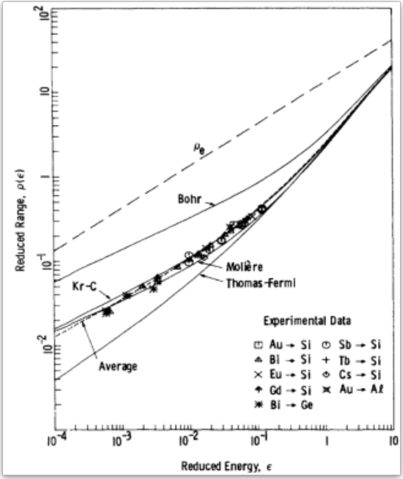

Figure: Wilson, Haggmark+ '76